Efficient photocatalytic proton-coupled electron-transfer reduction of O2 using a saddle-distorted porphyrin as a photocatalyst

	Emi Aoki, Wataru Suzuki, Hiroaki KOTANI, Tomoya ISHIZUKA, Hayato Sakai, Taku Hasobe, Takahiko KOJIMA
journal or publication title	Chemical communications
volume	55
number	34
page range	4925-4928
year	2019-05
	(C) The Royal Society of Chemistry 2019
URL	http://hdl.handle.net/2241/00157107

COMMUNICATION

Efficient photocatalytic proton-coupled electron-transfer reduction of O₂ by a saddle-distorted porphyrin as a photocatalyst

Emi Aoki,[a] Wataru Suzuki,[a] Hiroaki Kotani,[a] Tomoya Ishizuka,[a] Hayato Sakai,[b] Taku Hasobe,[b] Takahiko Kojima*[a]

Photocatalytic O₂ reduction reactions proceeded to produce H₂O₂ by a diprotonated saddle-distorted dodecaphenylporphyrin as a photocatalyst. The quantum yield (12%), the turnover number (3000 for 6 h), and the turnover frequency (500 h⁻¹) are achieved in photocatalytic systems based on free-base porphyrins for the first time. The photocatalytic reaction mechanism has been revealed by ns-laser flash photolysis and the kinetic analysis.

Oxygen reduction reaction (ORR) has been recognized as one of the most fundamental reactions in biological processes as performed by cytochrome *c* oxidase in respiration[1] and chemical technologies such as fuel cells.[2] In addition, hydrogen peroxide (H₂O₂) is a promising candidate for environmentally benign oxidizing reagents, bleaching, and an energy source of fuel cells as a two-electron reduced product in ORR (eqn 1).[3] In industry, H₂O₂ is manufactured by the anthraquinone process, which requires a hydrogen gas to reduce anthraquinone in the presence of a palladium catalyst.[4] Instead of the energy-consuming process using precious resources, alternative ORR catalysis for H₂O₂ production should be required to be constructed on the basis of photon energy without using precious metals.

$$O_2 + 2e^- + 2H^+ \longrightarrow H_2O_2 \qquad (1)$$
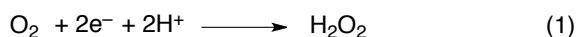
Toward this goal, extensive efforts have been devoted to the development of ORR catalysts for selective H₂O₂ production thermally[5] or photochemically[6] in the presence of acids without using noble metals. Especially, organocatalysts should be good candidates for proton-coupled O₂ reduction because of involvements of protons in the course of their redox reactions.[7] In addition, utilization of the visible light should be advantageous in terms of sustainable and environmental benign catalytic reactions.[3,6] Among organic photocatalysts, porphyrins are good candidates because of their rich redox-active properties and photochemical properties including strong absorption in a wide range of visible region.[8] However, there is no report on the use of a free-base porphyrin as a photocatalyst for ORR due to the high efficiency of energy transfer from the triplet excited state to molecular oxygen (O₂) to afford the singlet oxygen (¹O₂).[9] To avoid energy transfer to O₂, introduction of saddle-distortion to the porphyrin core should be effective because of the destabilization of the HOMO level, resulting lower triplet excited energy.[9,10] Among saddle-distorted porphyrins, a diprotonated saddle-distorted dodecaphenylporphyrin[11] (H₄DPP²⁺) has been selected as a photocatalyst in this study because the photodynamics and electron-transfer properties of H₄DPP²⁺ have been well understood.[12] Recently, we have reported that a water-soluble H₄DPP²⁺ derivative works as a photosensitizer for photocatalytic oxidation reactions in water.[13] Besides a role of photosensitizer, H₄DPP²⁺ has also acted as an electron acceptor to afford one-electron-reduced species (H₄DPP•⁺) due to the high reduction potential (E_{red} = −0.37 V *vs.* SCE)[12], which allows us to expect that H₄DPP•⁺ acts as a reducing agent for ORR. Judging from the characteristic properties of saddle-distorted porphyrins, photocatalytic ORR could be achieved by employing H₄DPP²⁺ as an ORR photocatalyst. Herein, we have developed a metal-free photocatalytic ORR system based on (H₄DPP²⁺)(Cl⁻)₂ (Fig. 1)[11b,14] in the presence of an electron donor and Brønsted acids to afford H₂O₂ efficiently and selectively.
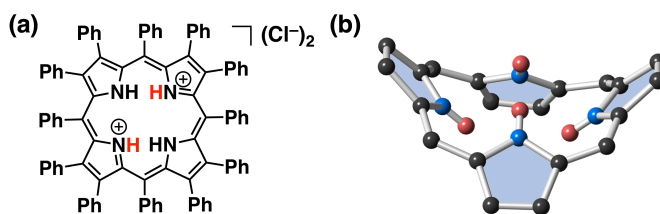

Fig. 1 (a) A chemical structure of H₄DPP²⁺(Cl⁻)₂ and (b) the structural model of H₄DPP²⁺ without peripheral phenyl groups.

a. Department of Chemistry, Faculty of Pure and Applied Sciences, University of Tsukuba and CREST (JST), 1-1-1 Tennoudai, Tsukuba, Ibaraki 305-8571, Japan
b. Department of Chemistry, Faculty of Science and Technology, Keio University, Yokohama, 223-8522, Japan

Photocatalytic ORR by H_4DPP^{2+} was performed in the presence of 10-methyl-9,10-dihydroacridine ($AcrH_2$) as a two-electron donor and carboxylic acids as a proton source in acetonitrile (MeCN) at 298 K. Upon photoirradiation (λ_{ex} = 480 nm) to a MeCN solution containing H_4DPP^{2+}, O_2, $AcrH_2$, and monochloroacetic acid (MCA), UV-vis spectral changes were observed as shown in Fig. 2. Absorption bands rose at 358 nm and 400 nm, which were derived from $AcrH^+$ as a two-electron-oxidized product of $AcrH_2$,[15] although the spectrum of H_4DPP^{2+} exhibiting the absorption maxima at 490 nm and 730 nm was almost intact. We quantified the amount of H_2O_2 as a two-electron reduced product of O_2 in ORR to be 99% yield based on $AcrH_2$ by an iodometry method, in which a reaction between NaI and H_2O_2 occurs to form I_3^- ion[5c,16] (Fig. S1 in the ESI†). In addition, the amount of $AcrH^+$ formed was consistent with that of H_2O_2 as shown in Fig. S2 in the ESI†. Therefore, the stoichiometry of photocatalytic ORR indicates that two-electron reduction of O_2 to form H_2O_2 proceeds quantitatively by eqn 2. It should be noted that photocatalytic ORR without H_4DPP^{2+} proceeded only slightly, although the rates of reactions without H_4DPP^{2+} depend on acids used as shown in Fig. S3 in the ESI† (also see below).
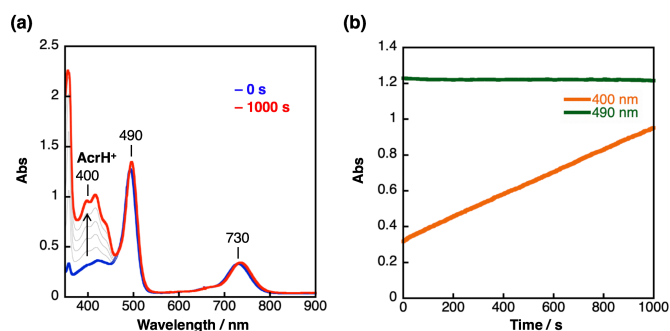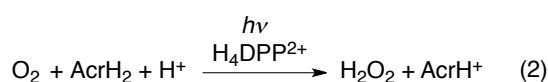
$$O_2 + AcrH_2 + H^+ \xrightarrow[H_4DPP^{2+}]{h\nu} H_2O_2 + AcrH^+ \qquad (2)$$

Fig. 2 (a) UV-vis spectral changes in photocatalytic ORR (λ_{ex} = 480 nm). Conditions: $[H_4DPP^{2+}]$ = 10 μM, $[AcrH_2]$ = 5 mM, [MCA] = 0.1 M, and $[O_2]$ = 0.29 mM in MeCN at 298 K. (b) The time profiles at 400 nm and 490 nm.

The time profile at 400 nm owing to $AcrH^+$ formation obeyed zero-order kinetics under the photocatalytic conditions (Fig. 2b). Thus, the observed zero-order rate (v, M s^{-1}) of $AcrH^+$ formation was determined from the linear slope of the plot at 400 nm. The zero-order-kinetics in $AcrH^+$ formation was also observed employing other acids such as trifluoroacetic acid (TFA), and dichloroacetic acid (DCA) with different values of v. The v values depend on the pK_a value of acids in MeCN[17] (Fig S4a in the ESI†), which is correlated with the positive shift of one-electron reduction potential of O_2 (Fig S4b in the ESI†). In addition, a linear-proportional relationship between v and the concentration of acids was also observed in the case of MCA as a proton source (Fig. 3a). Judging from these results, one proton is involved to accelerate ORR through proton-coupled electron transfer (PCET). When we changed the concentration of $AcrH_2$ ($[AcrH_2]$), the v value increased proportionately with

increasing $[AcrH_2]$ as shown in Fig. 3b. Such a linear-proportional relationship was also observed by changing light intensity (Fig. 3c).[18] In contrast, there is no dependence of v on $[O_2]$[15] (Fig. 3d), which indicates that the ORR rate law depends on light intensity, $[AcrH_2]$, and $[H^+]$. In this case, the kinetic equation was given by eqn 3.

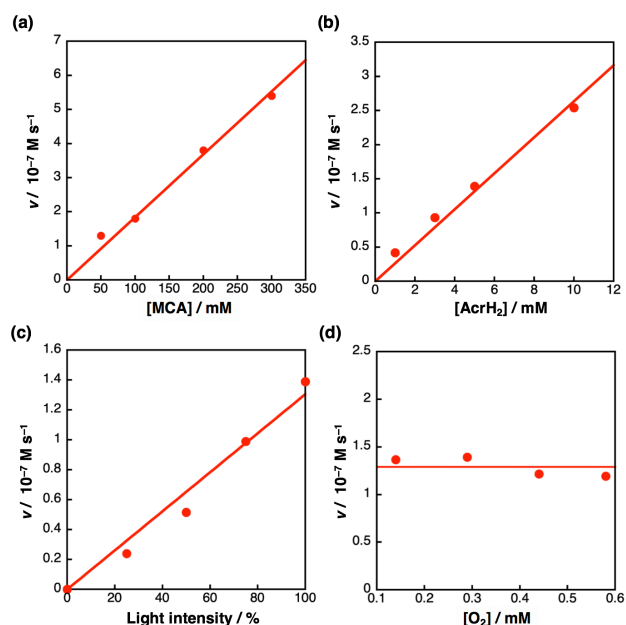$$v = \frac{d[AcrH^+]}{dt} = k_{cat}[^3(H_4DPP^{2+})^*][AcrH_2][H^+] \qquad (3)$$

Fig. 3 Plots of rates (v) of $AcrH^+$ formation vs. (a) [MCA] in the presence of 5.0 mM $AcrH_2$ and 0.29 mM O_2, (b) $[AcrH_2]$ in the presence of 0.1 M MCA and 0.29 mM O_2, (c) light intensity at 480 nm in the presence of 5.0 mM $AcrH_2$, 0.1 M MCA and 0.29 mM O_2, and (d) $[O_2]$ in the presence of 0.1 M MCA and 5.0 mM $AcrH_2$, under photocatalytic ORR conditions (λ_{ex} = 480 nm) in MeCN containing H_4DPP^{2+} (10 μM) at 298 K.

Under the optimized ORR conditions, the quantum yield (Φ) is determined using a ferrioxalate actinometer to be 12% and the turn-over number (TON) and the turnover frequency (TOF) of H_2O_2 production is also determined to be over 3000 for 6 h and 500 h^{-1} based on the amount of H_4DPP^{2+}, $[H_4DPP^{2+}]$, as shown in Fig S5 in the ESI†. Photocatalytic ORR using free-base porphyrins has been achieved for the first time.[19] In order to obtain a strong evidence for the photocatalytic performance, the requirement of visible light irradiation for H_2O_2 production was examined by repeating on/off cycles of the visible light irradiation. Fig. 4 clearly demonstrates that the photocatalytic ORR only proceeds during visible-light irradiation and stopped in the dark alternately. Thus, the possibility of thermal radical-chain mechanisms[15] could be ruled out based on the determination of the Φ value[20] and the light on-off experiments, confirming the indispensable role of visible light for the photocatalytic H_2O_2 production.

COMMUNICATION

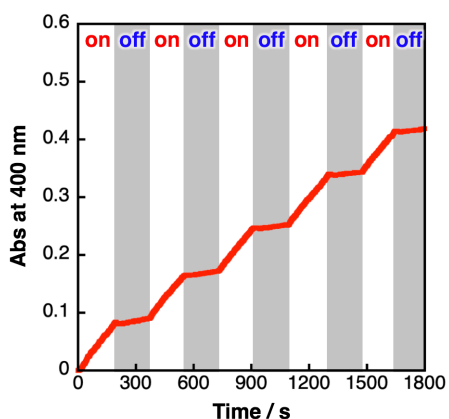**Fig. 4** Repeated experiments with or without photoirradiation under photocatalytic ORR conditions (λ_{ex} = 480 nm) in MeCN containing 10 μM H_4DPP^{2+}, 50 mM MCA, 3.0 mM $AcrH_2$, and 3.0 mM O_2 at 298 K.

To investigate the photocatalytic ORR mechanism by H_4DPP^{2+}, we performed nano-second laser flash photolysis (ns-LFP) under the similar reaction conditions to those described above. Upon photoirradiation at 532 nm to a deaerated MeCN solution of H_4DPP^{2+} containing trifluoroacetic acid (TFA) as a proton source, the transient absorption spectra of H_4DPP^{2+} showed an absorption band at 560 nm at 1.6 μs after laser excitation, indicating the formation of the triplet excited state of H_4DPP^{2+} ($^3(H_4DPP^{2+})^*$) via fast intersystem crossing from the singlet excited state of H_4DPP^{2+} ($^1(H_4DPP^{2+})^*$) (Fig. S6 in the ESI†).[12] Then, transient absorption spectra of H_4DPP^{2+} were measured in the presence of $AcrH_2$ to examine photoinduced electron transfer (ET) from $AcrH_2$ to $^3(H_4DPP^{2+})^*$ (Fig. 5). In contrast to the result in Fig. S6, transient absorption spectrum derived from $^3(H_4DPP^{2+})^*$ at 0.8 μs after laser excitation changed to a spectrum with a new absorption band at 520 nm (blue trace in Fig. 5), suggesting the photoinduced ET from $AcrH_2$ to $^3(H_4DPP^{2+})^*$ to form the one-electron reduced H_4DPP^{2+} ($H_4DPP^{\bullet+}$).[12] The decay time profile at 560 nm assigned to $^3(H_4DPP^{2+})^*$ coincides with the rise time profile at 520 nm due to $H_4DPP^{\bullet+}$ as shown in Fig. 5b. The second-order rate constant (k_{et}) of photoinduced ET from $AcrH_2$ to $^3(H_4DPP^{2+})^*$ was determined to be 5.4 x 10^6 M^{-1} s^{-1} by changing [$AcrH_2$] (Fig. S7 in the ESI†).

The rate constant (k_{O2}) of ET from $H_4DPP^{\bullet+}$ to O_2 was also determined by changing [O_2] as shown in Fig. S8 in the ESI†. The rate constant (k_{O2}) is calculated to be 3.4 x 10^6 M^{-1} s^{-1}, which is almost the same value in comparison to k_{et} (= 5.4 x 10^6 M^{-1} s^{-1}). The driving forces of ET ($-\Delta G_{et}$) for k_{et} ($-\Delta G_{et}$ = 0.30 eV) and k_{O2} ($-\Delta G_{et}$ = -0.06 eV) were determined from the difference between one-electron oxidation potential (E_{ox}) of $AcrH_2$ (E_{ox} = 0.81 V *vs.* SCE)[21] and one-electron reduction potential (E_{red}) of $^3(H_4DPP^{2+})^*$ (E_{red} = 1.11 V *vs.* SCE in MeCN), and that between E_{ox} of $H_4DPP^{\bullet+}$ (E_{ox} = -0.37 V) and O_2 in the presence of 10 mM TFA (E_{red} = -0.43 V). Judging from these $-\Delta G_{et}$ values, the k_{O2} value is larger than the expected value (~10^4 M^{-1} s^{-1}) from the Marcus parabola as described in the previous paper.[12] This large rate constant indicates that the O_2 reduction process is accelerated by the subsequent protonation of $O_2^{\bullet-}$ concertedly. This hypothesis is well consistent with the result of pK_a dependence on the photocatalytic ORR rate as described above (Fig S4 in the ESI†).

The proposed ORR mechanism has been shown in Scheme 1. Upon photoexcitation of H_4DPP^{2+} in the presence of $AcrH_2$ as an electron donor, photoinduced ET occurs to produce $H_4DPP^{\bullet+}$ with the expected k_{et} value determined by ns-LFP. Subsequently, PCET from $H_4DPP^{\bullet+}$ to O_2 is also observed in the presence of a proton source with a similar k_{O2} value in spite of the uphill $-\Delta G_{et}$ value estimated from the redox potentials of H_4DPP^{2+} and O_2. Thus, we can conclude that the fast ET and PCET processes performed by H_4DPP^{2+} allow us to construct the efficient photocatalytic ORR system.
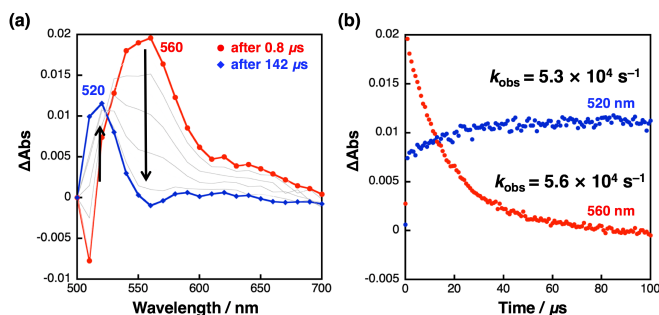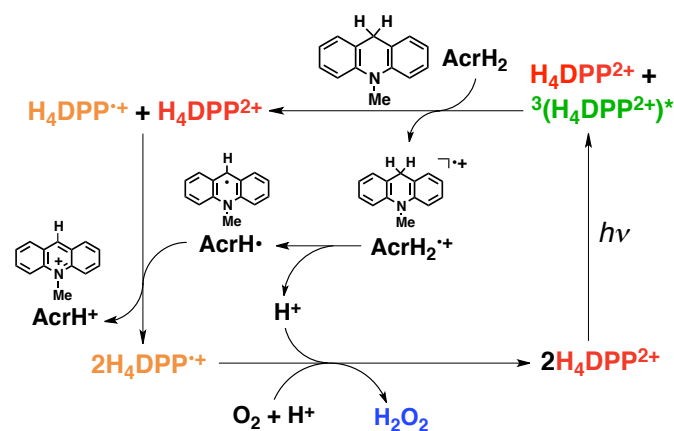

Fig. 5 (a) Transient absorption spectra of H_4DPP^{2+} (50 μM) in the presence of $AcrH_2$ (15 mM) and TFA (0.1 M) in deaerated MeCN at 298 K taken at 0.8 μs (red) and 142 μs (blue) after nano-second laser excitation at 532 nm. (b) The decay and rise time profiles at 520 nm. (blue) and 560 nm (red) in photoinduced ET from $AcrH_2$ to $^3(H_4DPP^{2+})^*$.

Scheme 1. Proposed photocatalytic ORR mechanism

In summary, we have succeeded in the development of the photocatalytic ORR system based on a diprotonated saddle-distorted porphyrin (H_4DPP^{2+}). The quantum yield of the photocatalytic system reaches 12% and the turnover number is determined to be over 3000 for 6 h. The reaction mechanism was clarified by nanosecond laser flash photolysis involving the formation of $H_4DPP^{\bullet+}$ as the key intermediate. The present study provides not only a new standard for photocatalytic ORR systems by porphyrin derivatives but also an application of a diprotonated porphyrin species as a reducing photocatalyst. Further applications of H_4DPP^{2+} derivatives are ongoing in our laboratory.

Conflicts of interest

There are no conflicts to declare.

Notes and references

1   (*a*) S. Ferguson-Miller and G. T. Babcock, *Chem. Rev.*, 1996, **96**, 2889-2907; (*b*) E. Kim, E. E. Chufán, K. Kamaraj and K. D. Karlin, *Chem. Rev.*, 2004, **104**, 1077-1133; (c) S. Yoshikawa, A. Shimada, *Chem. Rev.*, 2015, **115**, 1936-1989.

2   (*a*) J. Lee, B. Jeong and J. D. Ocon, *Curr. Appl. Phys.*, 2013, **13**, 309-321; (*b*) M. L. Pegis, C. F. Wise, D. J. Martin and J. M. Mayer, *Chem. Rev.*, 2018, **118**, 2340-2391.

3   S. Fukuzumi, *Joule,* 2017, **1**, 689-738.

4   J. M. Campos-Martin, G. Blanco-Brieva, and J. L. G. Fierro, *Angew. Chem., Int. Ed.,* 2006, **45**, 6962-6984.

5   (*a*) C. J. Chang, Z.-H. Loh, C. Shi, F. C. Anson and D. G. Nocera, *J. Am. Chem. Soc.,* 2004, **126**, 10013-10020; (*b*) T. Honda, T. Kojima and S. Fukuzumi, *J. Am. Chem. Soc.,* 2012, **134**, 4196-4206; (*c*) K. Mase, K. Ohkubo and S. Fukuzumi, *J. Am. Chem. Soc.,* 2013, **135**, 2800-2808; (*d*) I. Monte-Pérez, S. Kundu, A. Chandra, K. E. Craigo, P. Chernev, U. Kuhlmann, H. Dau, P. Hildebrandt, C. Greco, C. V. Stappen, N. Lehnert and K. Ray, *J. Am. Chem. Soc.,* 2017, **139**, 15033-15042; (*e*) Y.-H. Wang, M. L. Pegis, J. M. Mayer and S. S. Stahl, *J. Am. Chem. Soc.,* 2017, **139**, 16458-16461.

6   (*a*) T. Lazarides, I. Sazanovich, A. J. Simaan, M. C. Kafentzi, M. Delor, Y. Mekmouche, B. Faure, M. Réglier, J. A. Weinstein, A. G. Coutsolelos and T. Tron, *J. Am. Chem. Soc.,* 2013, **135**, 3095-3103; (*b*) S. Kato, J. Jung, T. Suenobu and S. Fukuzumi, *Energy Environ. Sci.,* 2013, **6**, 3756-3764; (*c*) K. Ohkubo and S. Fukuzumi, *Chem. Sci.,* 2013, **4**, 561-574.

7   (*a*) I. Hatay, B. Su, M. A. Méndez, C. Corminboeuf, T. Khoury, C. P. Gros, M. Bourdillon, M. Meyer, J.-M. Barbe, M. Ersoz, S. Zális, Z. Samec and H. H. Girault, *J. Am. Chem. Soc.,* 2010, **132**, 13733-13741; (*b*) S. Wu and B. Su, *Chem. Eur. J.* 2012, **18**, 3169-3173; (*c*) K. Mase, K. Ohkubo, Z. Xue, H. Yamada and S. Fukuzumi, *Chem. Sci.,* 2015, **6**, 6496-6504.

8   (*a*) K. M. Kadish and M. M. Morrison, *J. Am. Chem. Soc.,* 1976, **98**, 3326-3328; (*b*) D. Dolphin, in *The Porphyrins V3 & V5*; Academic Press, New York, 1978.

9   B. Röder, M. Büchner, I Rückmann and M. O. Senge, *Photochem. Photobiol. Sci.*, 2010, **9**, 1152–1158.

10 (*a*) J. A. Shelnutt, X. Z. Song, J. G. Ma, S. L. Jia, W. Jentzen and C. J. Medforth, *Chem. Soc. Rev.*, 1998, **27**, 31–41; (*b*) M. O. Senge, M. W. Renner, W. W. Kalisch and J. Fajer, *J. Chem. Soc., Dalton Trans.*, 2000, 381-385.

11 (*a*) C. J. Medforth, M. O. Senge, K. M. Smith, L. D. Sparks and J. A. Shelnutt, *J. Am. Chem. Soc.,* 1992, **114**, 9859-9869; (*b*) R. Harada and T. Kojima, *Chem. Commun.,* 2005, 716-718; (*c*) S. Fukuzumi, T. Honda and T. Kojima, *Coord. Chem. Rev.,* 2012, **256**, 2488-2502.

12 T. Nakanishi, K. Ohkubo, T. Kojima and S. Fukuzumi, *J. Am. Chem. Soc.,* 2009, **131**, 577-584.

13 T. Ishizuka, S. Ohkawa, H. Ochiai, M. Hashimoto, K. Ohkubo, H. Kotani, M. Sadakane, S. Fukuzumi and T. Kojima, *Green Chem*., 2018, **20**, 1975-1980.

14 Under the reaction conditions employed in this study, H_2DPP is completely diprotonated to be H_4DPP^{2+} and is not in the free-base form. See: W. Suzuki, H. Kotani, T. Ishizuka, Y. Shiota, K. Yoshizawa, *Chem. Commun.* 2017, **53**, 6359-6362.

15 S. Fukuzumi, M. Ishikawa and T. Tanaka, *J. Chem. Soc. Parkin Trans. 2,* 1989, 1037-1045.

16 S. Fukuzumi, S. Kuroda and T. Tanaka, *J. Am. Chem. Soc.,* 1985, **107**, 3020-3027.

17 K. Izutsu, in *Acid–Base Dissociation Constants in Dipolar Aprotic Solvents*, Blackwell Scientific Publications, Oxford, 1990.

18 The dependence of light intensity is accounted for the changing the amount of photons per unit area, which is related to the concentration of excited state of H_4DPP^{2+}.

19 A nonplanar free base porphyrin has been used as an organocatalyst in Michael addition of thiolates to electron-deficient olefins: M. Roucan, M. Kielmann, S. J. Connon, S. S. R. Bernhard and M. O. Senge, *Chem. Commun.,* 2018, **54**, 26-29.

20 M. A. Cismesia and T. P. Yoon, *Chem. Sci.*, 2015, **6**, 5426-5434.

21 S. Fukuzumi, Y. Tokuda, T. Kitano, T. Okamoto and J. Otera, *J. Am. Chem. Soc.,* 1993, **115**, 8960-8968.

TOC